Cyanide Coordination to Iron(III) Porphyrins and Covalently Linked Diiron(III) Diporphyrins†

Stanisław Wołowiec and Lechosław Latos-Grażyński*

Institute of Chemistry, University of Wrocław, 14 F. Joliot-Curie St., Wrocław 50 383, Poland

Received April 6, 1993®

The coordination of cyanide by diiron(III) diporphyrins in chloroform has been studied by ^{1}H NMR and ^{2}H NMR spectroscopy in order to determine the reaction pathway and intermediates. The diiron(III) diporphyrin of general formula $XFe^{III}TTPO(CH_2)_nOTTPFe^{III}X$ (X = Cl^-, Br^-, I^-; TTPO = 5-(*o*-(*m*-,*p*-)-hydroxy)-10,15,20-tritolylporphyrin dianion) has been synthesized. Two TTPO units are linked via diether moiety (n = 2 or 3) through *ortho*-, *meta*-, or *para*-positions of meso phenyls. The cyanide salts tetrabutylammonium cyanide [TBA][CN] and bis(triphenylphosphine)nitrogen(1+) cyanide [BPN][CN] have been used in NMR titrations. The formation of a high-spin, monocyano species has been established in the first reaction step for all systems under investigation. The pyrrole resonances appear at characteristic position at 70 ppm (293 K). The electronic structures of monocyano iron(III) complexes and of high-spin, five-coordinate halide diiron(III) diporphyrins are similar. The monocyano species are converted into low-spin μ-cyano-bridged diiron(III) complexes of the intra- or intermolecular structure as determined by diporphyrin geometry. Two different types of μ-cyano bridged species have been detected by ^{1}H and ^{2}H NMR and IR spectroscopy. Reaction of diiron(III) diporphyrin and cyanide in excess results in the formation of low-spin $[(CN)_2Fe^{III}TTPO(CH_2)_nOTTPFe^{III}(CN)_2]^{2-}$ complexes. The NMR results indicate that the effective C_s symmetry of the diporphyrin subunits is retained in the diiron(III) diporphyrins. The paramagnetic shifts of tricyano and tetracyano species are in a typical range for low-spin iron(III) porphyrins. The magnetic interaction between two paramagnetic centers of $\{[(CN)Fe^{III}TTPO(CH_2)_nOTTPFe^{III}(CN)](\mu\text{-}CN)\}^-$ is small as reflected by paramagnetic shift of pyrrole resonances. The characteristic connectivity patterns have been determined for pyrrole resonances of low-spin iron(III) diporphyrins by means of 2D COSY and NOESY ^{1}H NMR.

Introduction

Covalently linked dimeric metalloporphyrins can be designed to achieve the relative orientation of two metalloporphyrin units in a predictable manner.[1-6] The study of these molecules has been focused on several aspects of their chemistry where the intermetalloporphyrin distance and orientation are expected to determine the course of the process.

Covalently linked metallodiporphyrins were investigated in biomimetic studies of electron transfer and energy transfer in photosynthesis.[1-5] The ability of cobalt derivatives to catalyze the four-electron reduction of dioxygen to water was established.[7a] The "gable" metallodiporphyrins were investigated as local models for the low-potential cytochrome c_3 and as an example of an artificial allosteric system.[8] The potential biochemical and catalytic relevance of heterobinuclear systems led, in large part, to syntheses of heterometallodiporphyrins[7] and heterobimetallic porphyrins.[9] The interest in this field is stimulated by biochemistry of cytochrome *c* oxidase, where the cytochrome a_3–Cu_B heme iron–copper pair catalyzes the reduction of dioxygen to water.[10]

The covalently linked diporphyrins were challenging targets of organic chemistry, and a large variety of such systems were developed.[1-8,11] Depending on the nature of the bridging spacer, two major classes can be distinguished with a fixed or flexible structure of diporphyrins. The synthetic choice of the rigid link (links) allows fine tuning of the metalloporphyrin–metalloporphyrin interaction.

The flexible bridges result in less specific chemistry because the geometry of the substrate is not as rigorously determined by a rigid diporphyrin ligand. Some of the accessible configurations of the two porphyrin subunits are expected to suit the steric requirement of the reaction of interest. Coordination chemistry of iron(III) porphyrins should profit from investigations carried out for the covalently linked metalloporphyrins. An artificial allosteric effect described by Tabushi et al. was established for coordination of nitrogen bases, dioxygen, or carbon monoxide to iron(II), cobalt(II), or zinc(II) "gable" porphyrin.[8] In contrast to regular iron(II) porphyrin, formation of a five-coordinate complex was favored over the six-coordinate one.[8c,d]

The work described here involves detection of species formed by the addition of cyanide to high-spin, covalently linked diiron(III) diporphyrin complexes.[55] The cyanide anion is frequently

† Abbreviations: [TTP*o*O$(CH_2)_2$O*o*TTP], tetraanion of 5,10,15-tri-*p*-tolyl-20-[2-[2-[*o*-(10,15,20-tri-*p*-tolylporphinyl)phenoxy]ethoxy]phenyl]-porphyrin; [TTP*o*O$(CH_2)_3$O*o*TTP], tetraanion of 5,10,15-tri-*p*-tolyl-20-[2-[3-[*o*-(10,15,20-tri-*p*-tolylporphinyl)phenoxy]propoxy]phenyl]porphyrin; [TTP*m*O$(CH_2)_3$O*m*TTP], tetraanion of 5,10,15-tri-*p*-tolyl-20-[3-[2-[*m*-(10,15,20-tri-*p*-tolylporphinyl)phenoxy]ethoxy]phenyl]porphyrin; [TTP*p*O$(CH_2)_3$O*p*TTP], tetraanion of 5,10,15-tri-*p*-tolyl-20-[4-[3-[*p*-(10,15,20-tri-*p*-tolylporphinyl)-phenoxy]propoxy]phenylporphyrin; [TTP*o*O$(CH_2)_2$O*o*TFP], tetraanion of 5,10,15-tri-*p*-tolyl-20-[2-[2-[*o*-(10,15,20-tri-*p*-fluorophenylporphinyl)phenoxy]ethoxy]phenyl]porphyrin; (TPP), dianion of 5,10,15,20-tetraphenylporphyrin; (TMP), dianion of 5,10,15,20-tetramesitylporphyrin; [TBA][CN], tetrabutylammonium cyanide; [BPN][CN], bis(triphenylphosphine)nitrogen(1+) cyanide.

® Abstract published in *Advance ACS Abstracts,* July 1, 1994.

(1) Dolphin, D.; Hiom, J.; Pain, J. B., III. *Heterocycles* **1981**, *16*, 417.
(2) Wasielewski, M. R. In *Photoinduced Electron Transfer. Part A*; Fox, M. A., Chanon, M., Eds. Elsevier: Amsterdam, 1988; pp 161–206.
(3) Sessler, J. L.; Johnson, M. R.; Lin, T.-Y.; Creager, S. E. *J. Am. Chem. Soc.* **1988**, *110*, 3659.
(4) Meier, H.; Kobuke, Y.; Kugimiya, S. *J. Am. Chem. Soc.* **1989**, *111*, 923.
(5) Dixon, D. B.; Kumar, V. *New J. Chem.* **1992**, *16*, 555 and references cited therein.
(6) Eaton, S.; Eaton, G. R.; Chang, C. K. *J. Am. Chem. Soc.* **1985**, *107*, 3177.
(7) (a) Collman, J. P.; Hutchison, J. E.; Lopez, M. A.; Tabard, A.; Guilard, R.; Seok, W. K.; Ibers, J. A.; L'Her, M. *J. Am. Chem. Soc.* **1992**, *114*, 9869. (b) Collman, J. P.; Wagenknecht, P. S.; Hutchison, J. E.; Lewis, N. S.; Lopez, M. A.; Guilard, R.; L'Her, M.; Bothner-By, A. A.; Mishra, P. K. *J. Am. Chem. Soc.* **1992**, *114*, 5654. (c) Guilard, R.; Lopez, M. A.; Tabard, A.; Richard, P.; Lecomte, C.; Brandes, S.; Hitchison, J. E.; Collman, J. P. *J. Am. Chem. Soc.* **1992**, *114*, 9877.
(8) (a) Tabushi, I.; Sasaki, T. *J. Am. Chem. Soc.* **1983**, *105*, 2901. (b) Tabushi, I.; Kugimiya, S.; Kinnaird, M. G.; Sasaki, T. *J. Am. Chem. Soc.* **1985**, *107*, 4192. (c) Tabushi, I.; Kugimiya, S.; Sasaki, T. *J. Am. Chem. Soc.* **1985**, *107*, 5159. (d) Tabushi, I.; Kugimiya, *J. Am. Chem. Soc.* **1986**, *108*, 6926. (e) Tabushi, I. *Pure Appl. Chem.* **1988**, *60*, 581.
(9) Bulach, V.; Mandon, D.; Weiss, R. *Angew. Chem., Int. Ed. Engl.* **1991**, *30*, 572.
(10) Malmström, B. O. G. *Chem. Rev.* **1990**, *90*, 1247.
(11) Landrum, T. J.; Grimmett, D.; Haller, K. J.; Scheidt, W. R.; Reed, C. A. *J. Am. Chem. Soc.* **1981**, *103*, 2640.

0020-1669/94/1333-3576$04.50/0

used to convert high-spin iron(III) porphyrins or hemoproteins to the low-spin state.[12-14] Equilibrium studies demonstrated the stepwise binding of cyanide to iron(III) porphyrins via intermediary low-spin, six-coordinate monocyano species in coordinating solvents or in presence of nitrogen bases.[15-22] The Fe–CN group is essentially linear in cyano and dicyano iron(III) tetraphenylporphyrin complexes[23] but kinked binding was established in a highly hindered dicyanoiron(III) basket-handle porphyrin complex.[24] The autoreduction of iron(III) porphyrin by cyanide was demonstrated.[20b,c]

Cyanide is a common ligand in transition metal complexes. It coordinates through the carbon to a single metal center (M–CN) or bridges two metals:[25]

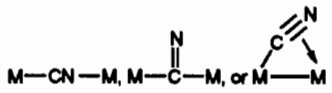

To our knowledge, the dimeric μ-cyano-bridged iron(III) porphyrins are unknown, but it was shown that coordinated cyanide acts as a Lewis base or a hydrogen bond acceptor.[19,20a] Proximity of two coordinating centers in covalently linked diiron diporphyrins should increase the chances for μ-cyano bridge formation.

^{1}H NMR spectroscopy provides a uniquely useful probe for studying the structure of covalently bridged diiron(III) diporphyrins in solution.[26] The hyperfine shift patterns are particularly sensitive to the spin, ligation, and oxidation states of the metal. For the complexes derived from symmetrical tetraphenylporphyrin, the presence of a substituent on one of four phenyl rings reduces symmetry to at most C_s, and thereby introduces a greater complexity of their NMR spectra.

Here we report a detailed examination of the ^{1}H NMR spectra of respective cyano complexes of covalently bridged diiron(III) diporphyrins. Included in these analyses are cross-correlations obtained from 2D NMR spectroscopy (COSY and NOESY) for paramagnetic systems.[27]

Results and Discussion

^{1}H NMR Characterization of Free Base Porphyrins. Diporphyrins investigated contain two tetraphenylporphyrin units covalently linked in the *ortho*, *meta*, or *para* positions of meso phenyls by a diether bridge. Two basic conformations of the diporphyrins substituted at *ortho* and *meta* positions for diporphyrin and its metal complexes, as previously considered,[28,29] are presented in Figure 1 (for the *ortho*-bridged species). The presence of the phenyl substituent lowers the symmetry of the porphyrin unit to C_s and renders four pyrrole positions nonequivalent in the ^{1}H NMR spectra of diporphyrins and respective dimetallic complexes. The chemical shifts of diporphyrins include the contribution of the external ring current effect. This provides an indication of the diporphyrin configuration.[30] The chemical shifts of monomeric mono-substituted porphyrins are taken to be the convenient monomeric reference; selected values are collected in Table 1. In the series studied we have observed noticeable external contribution in the neighborhood of the link only in the case of *ortho*-linked diporphyrins. The largest ring current shift has been determined for the *ortho*-substituted phenyl but pyrrole shifts were only slightly influenced (Figure 2). We conclude that the open configuration of diporphyrins prevails in the solution, with the largest accessible porphyrin–porphyrin distance.

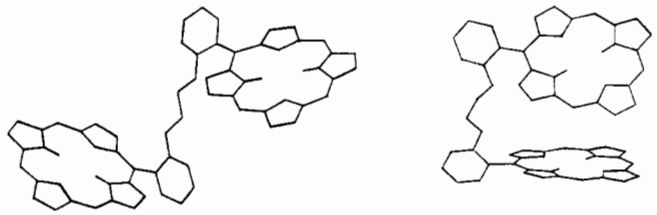

Figure 1. Drawing of the folded and extended conformations of *o*-ethylene diether-linked diporphyrin. Phenyl rings and atom labeling are omitted for the sake of clarity.

Characterization of High-Spin Iron(III) Diporphyrins. The ^{1}H NMR spectra of high-spin diiron(III) diporphyrin complexes of general formula $XFe^{III}TTPO(CH_2)_nOTTPFe^{III}X$ ($X = Cl^-$, Br^-, I^-) resemble closely those obtained for monomeric analogs (R-OTTP)$Fe^{III}X$. The most characteristic features are presented in Figures 3 (trace a) and 4 (trace a). Three isomeric forms are expected for *ortho*- and *meta*-linked dimers, depending on the coordination side of axial ligands (*endo*, *endo*; *endo*, *exo*; *exo*, *exo*) because the bridge renders the two faces of the core nonequivalent. It has been expeditious to examine the data of bromide and iodide forms where the resolution is optimal.[26] The isotropic shift of high-spin iron(III) porphyrins is usually rationalized in terms of contact and dipolar shifts.[31] The dipolar contribution is geometry dependent[26] and additive. One can expect to observe the external dipolar shift which adds to the internal one in diiron(III) diporphyrins. The external dipolar contribution should reflect the geometry of diiron(III) diporphyrin. Such contribution is not visible in ^{1}H NMR spectra of diiron(III) diporphyrins studied in this paper even for the iodide derivative with the largest dipolar shifts.[31] This suggests a domination of the extended structures or the eclipsed configuration, which locate the two porphyrins too far away to produce measurable dipolar contributions. Electronic spectra of iron(III) diporphyrins are very similar to their monomeric counterparts; this confirms structural conclusion based on the ^{1}H NMR data. The asymmetry imposed by the *ortho* substitution is not sufficient to split the pyrrole resonance at 80 ppm into the expected four lines. The

(12) La Mar, G. N.; Viscio, D.; Smith, K.; Caughey, W. S.; Smith, M. L. *J. Am. Chem. Soc.* **1978**, *100*, 8085.
(13) Rajarathnam, K.; La Mar, G. N.; Chiu, M. L.; Sligar, S. G. *J. Am. Chem. Soc.* **1992**, *114*, 9048.
(14) Czechowski, F.; Latos-Grażyński, L. *Naturwissenschaften* **1990**, *77*, 578.
(15) Wang, J.-T.; Yeh, H. J. C.; Johnson, D. F. *J. Am. Chem. Soc.* **1978**, *100*, 3021.
(16) (a) Goff, H.; Morgan, L. O. *Inorg. Chem.* **1976**, *15*, 2069. (b) Goff, H. *J. Am. Chem. Soc.* **1977**, *99*, 7723.
(17) (a) Barnitz, V.; Leusing, D. L. *J. Inorg. Biochem.* **1991**, *43*, 336. (b) Weinraub, D.; Peretz, P.; Faraggi *J. Chem. Phys.* **1982**, *86*, 1839. (c) Arifuku, F.; Ujimoto, K.; Kurihara, H. *Bull. Chem. Soc. Jpn.* **1986**, *59*, 149.
(18) (a) Dixon, D. W.; Barbush, M.; Shirazi, A. *J. Am. Chem. Soc.* **1984**, *106*, 4638. (b) Dixon, D. W.; Barbush, M.; Shirazi, A. *Inorg. Chem.* **1985**, *24*, 1081. (c) Hwang, Y. C.; Dixon, D. W. *Inorg. Chem.* **1986**, *25*, 3716.
(19) Morishima, I.; Inubushi, T. *J. Am. Chem. Soc.* **1978**, *100*, 3568.
(20) (a) Frye, J. S.; La Mar, G. N. *J. Am. Chem. Soc.* **1975**, *97*, 3652. (b) del Gaudio, J.; La Mar, G. N. *J. Am. Chem. Soc.* **1976**, *98*, 3014. (c) La Mar, G. N.; del Gaudio, J. *Adv. Chem. Ser.* **1977**, *162*, 207. (d) La Mar, G. N.; Del Gaudio, J.; Frye, J. S. *Biochim. Biophys. Acta* **1977**, *498*, 422.
(21) Traylor, T. G.; Mitchell, M. J.; Ciccone, J. P.; Nelson, S. *J. Am. Chem. Soc.* **1982**, *104*, 4986.
(22) Balch, A. L.; Cornman, C. R.; Latos-Grażyński, L.; Olmstead, M. M. *J. Am. Chem. Soc.* **1990**, *112*, 7552.
(23) (a) Scheidt, W. R.; Haller, K. J.; Hatano, K. *J. Am. Chem. Soc.* **1980**, *102*, 3017. (b) Scheidt, W. R.; Haller, Ja Lee, Y.; Luangdilok, W.; Haller, K. J.; Anzai, K.; Hatano, K. *Inorg. Chem.* **1983**, *22*, 389.
(24) Schappacher, M.; Fischer, J.; Weiss, R. *Inorg. Chem.* **1989**, *28*, 391.
(25) Jun, H.; Young, V. G., Jr.; Angelici, R. J. *J. Am. Chem. Soc.* **1992**, *114*, 10064 and references cited therein.
(26) La Mar, G. N.; Walker, F. A. In *The Porphyrins*; Dolphin, D., Ed.; Academic Press: New York, 1979; Vol. IV, p 61.
(27) Keating, K. A.; de Ropp, J. S.; La Mar, G. N.; Balch, A. L.; Shiau, F.-Y. *Inorg. Chem.* **1991**, *30*, 3258.
(28) (a) Maillard, P.; Krausz, P.; Giannotti, C.; Gaspard, S. *J. Organomet. Chem.* **1980**, *197*, 295. (b) Maillard, P.; Gaspard, S.; Krausz, P.; Giannotti, C. *J. Organomet. Chem.* **1981**, *212*, 185. (c) Krausz, P.; Giannotti, C. *J. Chim. Phys.* **1983**, *80*, 299.
(29) (a) Regev, A.; Galili, T.; Levanon, H.; Harriman, A. *Chem. Phys. Lett.* **1986**, *131*, 140. (b) Huber, M.; Galili, T.; Möbius, K.; Levanon, H. *Israel J. Chem.* **1989**, *29*, 65.
(30) Uemori, Y.; Nakatsubo, A.; Imai, H.; Nakagawa, S.; Kyuno, *Inorg. Chem.* **1992**, *31*, 5164.
(31) (a) La Mar, G. N.; Eaton, G. R.; Holm, R. H.; Walker, F. A. *J. Am. Chem. Soc.* **1973**, *95*, 63. (b) Behere, D. V.; Birdy, R.; Mitra, S. *Inorg. Chem.* **1982**, *21*, 2432.

Table 1

diporphyrin	chemical shift difference[a] (ppm)							
	pyrrolic resonances			substituted phenyl resonances				
	$\Delta pyrr_{1,2}$	$\Delta pyrr_3$	$\Delta pyrr_4$	Δo_5	Δo_6	Δm_5	Δm_6	Δp
$H_2TTPoO(CH_2)_2OoTTPH_2$[b]	−0.01	−0.12	−0.29	−0.45	−	−1.29	−1.48	−1.51
$H_2TTPoO(CH_2)_3OoTTPH_2$[b]	+0.01	−0.11	−0.24	−0.28	−	−0.76	−1.53	−0.72
$H_2TTPmO(CH_2)_3OmTTPH_2$[c]	+0.02	+0.02	−0.02	−0.04	+0.04	−0.04	−	0.00

[a] Negative sign of difference means upfield shift, pyrrolic resonances 1 and 2 belong to A_2 system and resonances 3 and 4 originate from an unequivalent pair of β-H pyrrolic hydrogens in cis position to substituted phenyl. The notation of phenyl resonances has been depicted in Figure 2. [b] Related to 2-bromoethylO*o*TTPH$_2$. [c] Related to 3-bromopropylO*m*TTPH$_2$.

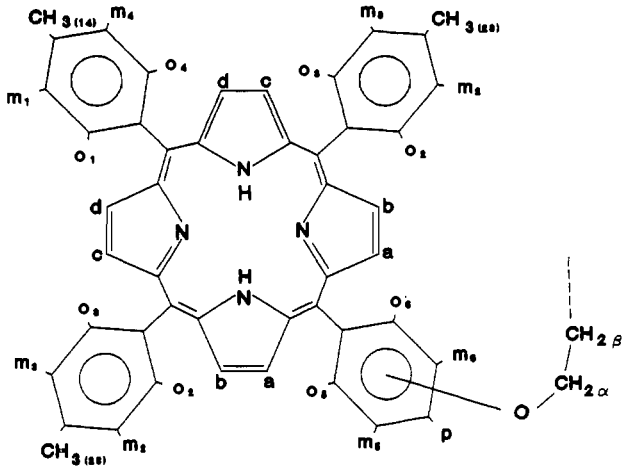

Figure 2. Numbering scheme for diporphyrins used throughout this paper. The bridging ethylene protons are labeled as $CH_{2(b)}$.

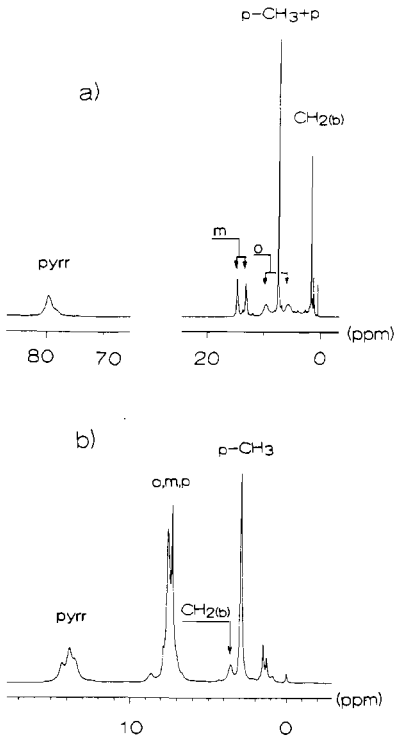

Figure 3. ^{1}H NMR spectra (293 K, $CDCl_3$): (a) BrFe^{III}TTP*o*O-$(CH_2)_2$O*o*TTPFe^{III}Br; (b) [Fe^{III}TTP*o*O$(CH_2)_2$O*o*TTPFe^{III}](μ-O). Abbreviations used in all figures: pyrr, pyrrole resonances; o, ortho, m, meta, and *p* para resonances of meso phenyl rings.

influence of the intrinsic asymmetry of diiron(III) diporphyrin on the ^{1}H NMR spectra is demonstrated for the (μ-oxo)diiron(III) complex [Fe^{III}TPP*o*O$(CH_2)_2$O*o*TTPFe^{III}]O where three pyrrole resonances of 1:2:1 intensities are present at 13 ppm, i.e. the position expected for μ-oxo-bridged iron(III) porphyrins.[26,31] (Figure 3, trace b)

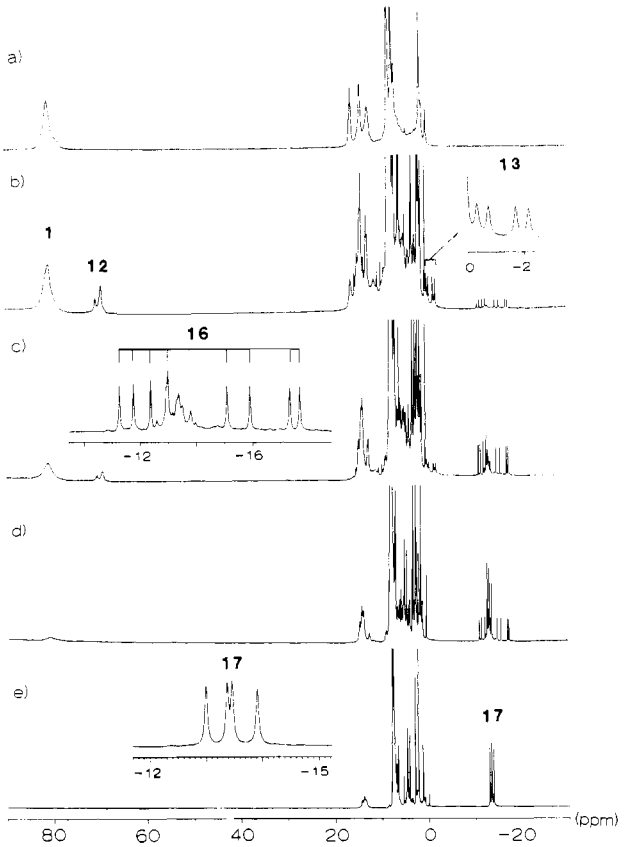

Figure 4. ^{1}H NMR titration of IFe^{III}TTP*o*O$(CH_2)_2$O*o*TTPFe^{III}I with [BPN][CN] (293 K, $CDCl_3$): (a) the starting complex; (b) 0.6, (c) 1, (d) 1.7, and (e) 2.1 equiv of cyanide per metal ion added. Only pyrrole resonances are labeled. Pyrrole resonance assignments to specific species in this and following figures refer to Scheme 1.

Cyanide Coordination to *ortho*-Linked Diiron(III) Diporphyrins. Addition of cyanide to high-spin iron(III) porphyrins results in a conversion to a low-spin state. The process usually required a polar solvent and addition of potassium cyanide.[12-21,23]

All titrations in this paper have been carried out in chloroform. Two convenient sources of cyanide have been used: [TBA][CN] and [BPN][CN]. The latter cyanide source was used in cases where the analysis of the 0–5 ppm region was required because [BPN][CN] is transparent in this part of the spectrum. The general proposed pathway of cyanide coordination by iron(III) diporphyrins is presented in Scheme 1.

We have assumed that (i) cyanide binds to iron(III) preferably via the cyanide carbon end, (ii) both associative and dissociative pathways are operating, and (iii) only 0, 1-, and 2- charged species are formed. The side reactions, i.e. reduction of Fe(III) to Fe(II) by cyanide, followed by reaction of Fe(II) and oxygen, or reactions of hydrolysis with trace water, both leading to μ-oxo species, are not included in Scheme 1. The species identified in the course of experiments are indicated by boxes.

The most characteristic features in the ^{1}H NMR spectra are demonstrated in Figures 4 and 5 and Table 2. The isotropic shift

Scheme 1

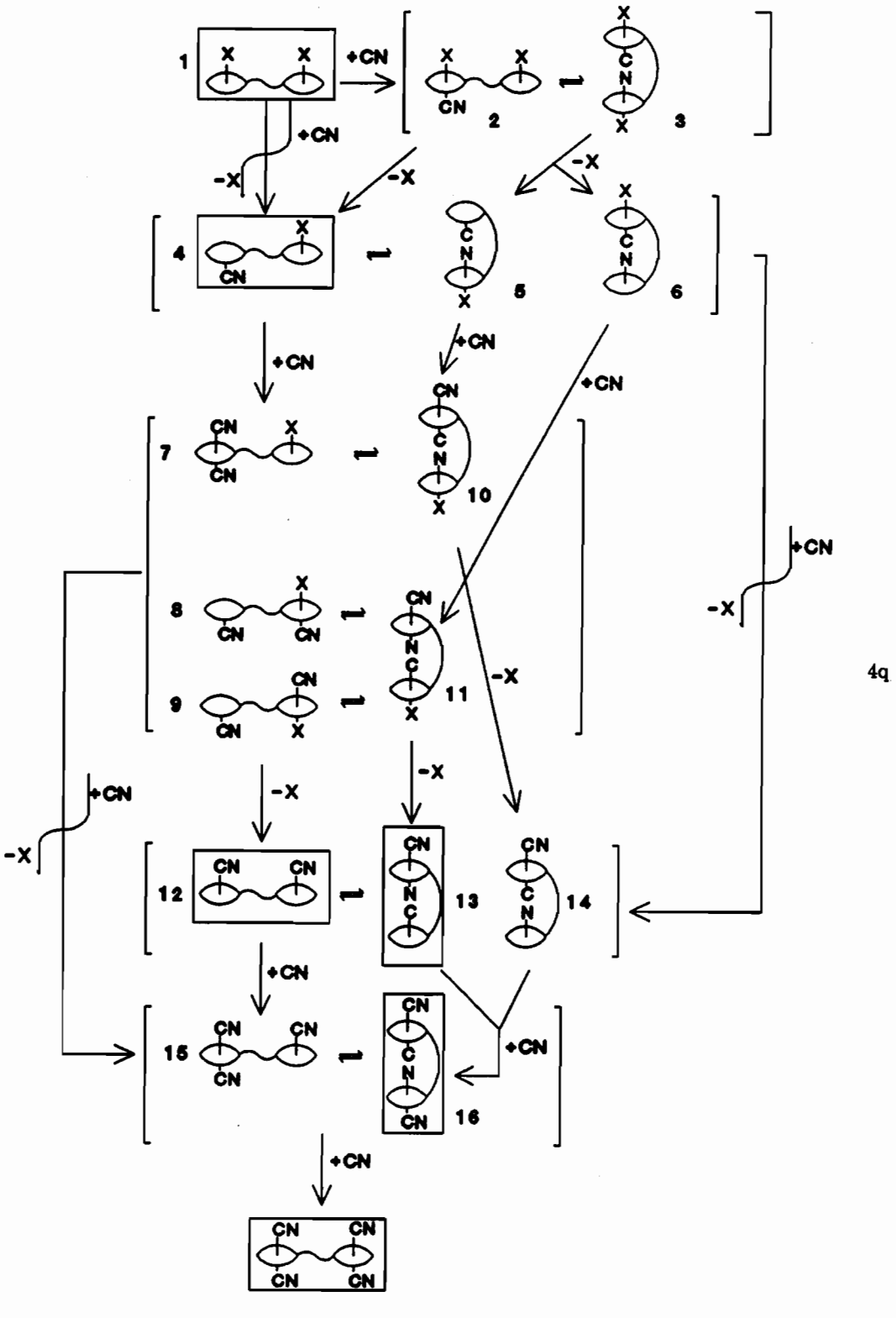

of the cyano species does not depend on the identity of the axial ligand in the starting high-spin diiron(III) diporphyrin. This leads to the conclusion that they are absent in the coordination sphere in the dominating, cyanide-containing species. The preference for iodide complexes as the titration substrates has been dictated by the fact that in the series studied Cl^-, Br^-, and I^-, the latter is the softest ligand and its replacement by cyanide should be the easiest. Titration of mixtures of chloro and iodo complexes has shown that the iodo complex reacts preferentially with cyanide.

The characteristic pyrrole resonances, whose positions reflect the spin/ligation state of the iron, have been labeled in the spectra according to Scheme 1, and the specific reason for the assignment is outlined later on. The effect of addition of cyanide to IFe^{III}-$TTPoO(CH_2)_2OoTTPFe^{III}I$ is shown in Figure 4. Trace a shows the spectrum of the original iron(III) complex in chloroform-*d* at 293 K, while traces b–e show the same sample after subsequent additions of cyanide equivalents. Comparison of the ^2H NMR spectrum of $IFe^{III}TTPoO(CH_2)_2OoTPPFe^{III}I$-$d_{16}$ with the corresponding trace, obtained from the ^1H NMR titration, confirmed

Table 2

(a) Complexes **17** and **16**

starting complex	chemical shift (ppm)[b]											
	17				**16 (16′)**							
ClFeTTP*o*O(CH$_2$)$_2$O*o*TTPFeCl	−13.29	−13.56	−13.96	−14.88	−11.98	−12.30	−12.86	−13.65	−15.16	−15.68	−17.34	−17.87
BrFeTTP*o*O(CH$_2$)$_2$O*o*TTPFeCl	−13.30[a]	−13.64[b]	−13.98[a]	−14.22[b]	−12.03	−12.39	−12.89	−13.68	−15.24	−15.74	−17.40	−17.93
IFeTTP*o*O(CH$_2$)$_2$O*o*TTPFeI												
titration with [TBA][CN]	−13.30	−13.63	−13.98	−14.24	−12.07[a]	−12.39[a]	−12.97[b]	−13.65[b]	−15.32[c]	−15.86[d]	−17.53[c]	−18.06[d]
titration with [BPN][CN][a]	−13.01	−13.39	−13.47	−13.93	−11.25	−11.75	−12.36	−12.99	−15.07	−15.90	−17.33	−17.69
BrFeTTP*o*O(CH$_2$)$_3$O*o*TTPFeBr	−13.13	−13.63	−13.87	−14.67	−9.82	−10.47	−10.57	−11.58	−14.58	−14.90	−17.02	−17.37
IFeTTP*o*O(CH$_2$)$_2$O*o*TFPFeI					−11.60[a]	−11.74[a]	−12.26[b]	−12.88[c]	−15.04[c]	−15.35[b]	−16.09[d]	−16.19[d]
					−12.96[e]	−13.18[f]	−13.22[g]	−14.14[h]	−17.10[e]	−17.69[f]	−17.82[h]	−18.29[g]
BrFeTTP*m*O(CH$_2$)$_3$O*m*TTPFeBr	−12.65	−13.42	−13.52	−13.81								
BrFeTTP*p*O(CH$_2$)$_3$O*p*TTPFeBr	−13.6											
(TPP)FeI												
titration with [TBA][CN]	−14.88				−13.08				−16.40			
titration with [BPN][CN]	−14.07				−12.37				−16.16			
(TMP)FeI	−12.15											

(b) Complex **13**

starting complex	chemical shift (ppm)[b] for **13** (**13′**)			
BrFeTTP*o*O(CH$_2$)$_2$O*o*TTPFeBr	−0.39	−0.79	−1.82	−2.25
IFeTTP*o*O(CH$_2$)$_2$O*o*TTPFeI				
titration with [TBA][CN]	−0.54[a]	−0.90[a]	−1.92[b]	−2.38[b]
titration with [BPN][CN]	−0.31	−0.71	−1.70	−2.15
IFeTTP*o*O(CH$_2$)$_2$O*o*TFPFeI				
major species	−1.50	−2.08	−3.30	−3.30
minor species	0.33	0.02	−1.08	−1.50

[a] All other titrations were done with [TBA][CN]. [b] a–h denote connectivities between corresponding β-pyrrolic hydrogens (from COSY experiments, see Figure 10).

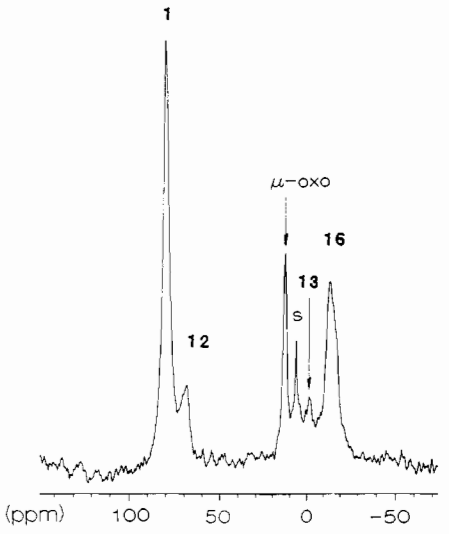

Figure 5. ^{2}H NMR spectrum of IFe^{III}TTP*o*OCH$_2$)$_2$O*o*TTPFe^{III}I-d_{16} after the addition of 0.8 equiv of [BPN][CN] (293 K, $CHCl_3$).

the assignment of pyrrole resonances (Figures 4 and 5). Trace e of Figure 4 shows the ^{1}H NMR spectrum after the addition of 2.1 equiv of cyanide per iron(III) porphyrin moiety. Four equally intense resonances are readily distinguished which are accompanied by respective phenyl resonances in the 0–8 ppm region. The split of pyrrole resonances results from the monosubstitution of one of the phenyl rings which imposes an effective C_s symmetry on each iron porphyrin moiety. Trace b of Figure 4 shows the ^{1}H NMR spectrum obtained after addition of 0.6 equiv of cyanide to a solution of IFe^{III}TTP*o*O(CH$_2$)$_2$O*o*TTPFe^{III}I. Pyrrole resonances, which appear in the downfield region, are indicative of the formation of a new high-spin iron(III) complex. These resonances are accompanied by corresponding *meta* resonances of meso phenyl in the 12–10 ppm region. At this concentration of cyanide the pyrrole resonances of a low-spin species are also encountered (Figure 4, trace b). The predominate low-spin species has pyrrole resonances in the 0 to −5 ppm region. Observation of the ^{2}H NMR spectrum with the d_{16} derivative confirms that these are pyrrole resonances (Figure 5). At this stage of the discussion we would like to point out their extremely small isotropic shifts. This species has been found only for the *ortho*-linked diporphyrins with the ethylene bridge. A side reaction resulting in formation of μ-oxo-bridged diiron(III) complexes has been noticed, as indicated by growth of a characteristic pyrrole resonance at 13 ppm. When cyanide concentration is increased to 1:1 equiv per metal ion (Figure 4, trace c) the formation of another low-spin species with an unique pattern of eight-pyrrole resonances is observed. The pattern reflects a dinuclear structure of this form with three cyanide ligands coordinated to the two iron(III) atoms of one diiron(III) diporphyrin (Scheme 1). One of the cyanide ligands acts as a bridge, as confirmed by an IR titration.[32,33] Two separate sets of four pyrrole resonances due to the different axial ligation have been found (NC–Fe–CN versus NC–Fe–NC) in **16**. The spectral patterns seen in Figure 4 can be compared to those of other diiron(III) diporphyrins with the

(32) The titration of IFe^{III}TTP*o*O(CH$_2$)$_2$O*o*TTPFe^{III}I and (TMP)Fe^{III}I with cyanide has been followed by IR spectroscopy. The formation of the μ-cyano bridge is expected in the first case but less probable in the second one. It was determined for series of μ-cyano-bridged dimetallic complexes that bridging causes an electron withdrawal from the lowest σ* orbital, effectively increasing both the cyanide bond order and stretching frequency.[33] In case of titration of IFe^{III}TTP*o*O(CH$_2$)$_2$-O*o*TTPFe^{III}I with [TBA][CN], two new bands are observed at 2203 and 2109 cm^{-1} after addition of less than 1 equiv of cyanide. The gradual increase of cyanide concentration resulted first in increase, followed by disappearing of the band at 2203 cm^{-1}. The intensity of the second one prevailed till the end of titration. On basis of the titration and the expected relation between energy of terminal and bridging cyanide stretches, we have assigned the band at 2203 cm^{-1} to the bridging cyanide and the band at 2109 cm^{-1} to the terminal one.[33d] No CN$^-$ stretching at wavenumbers higher than 2140 cm^{-1} has been observed in the (TMP)-Fe^{III}I titration as the respective diiron species is not formed. Thus, the infrared data confirmed the formation of μ-cyano bridged species for diiron(III) diporphyrins.

(33) (a) Doorn, S. K.; Hupp, J. T. *J. Am. Chem. Soc.* **1989**, *111*, 1143. (b) Bignozzi, C. A.; Roffia, S.; Chiorbolli, C.; Davila, J.; Indelli, M. T.; Scandola, F. *Inorg. Chem.* **1989**, *28*, 4350. (c) Copper, J. B.; Vess, T. M.; Kalsbeck, W. A.; Wertz, D. W. *Inorg. Chem.* **1991**, *30*, 2286. (d) De Castelló, R. A.; Mac-Coll, C. P.; Haim, A. *Inorg. Chem.* **1971**, *10*, 203.

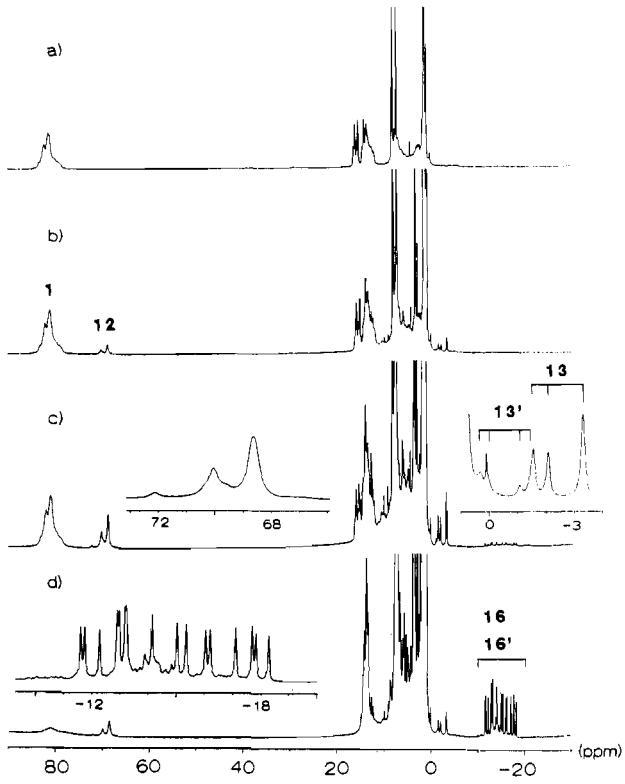

Figure 6. ^{1}H NMR titration of IFe^{III}TTP*o*O(CH$_2$)$_2$O*o*TFPFe^{III}I with [TBA][CN] (293 K, $CDCl_3$): (a) the starting complex, (b) 0.3, (c) 0.7, and (d) 1.1 equiv of cyanide per metal ion added. Insert in trace d presents pyrrole resonances of μ-cyanide bridged species **16** and **16'**.

similar geometry but with the different substitution at phenyl rings of two moieties IFe^{III}TTP*o*O((CH$_2$)$_2$O*o*TFPPFe^{III}I (β-methyl vs β-F in the studied molecule) (Figure 6). Such a modification results in some differences in the coordinating properties and in the isotropic shift of two subunits. We have observed also two isomeric forms for each undertitrated species. The most spectacular results have been obtained for triscyano, μ-cyano bridged species (**16**, **16'**) where the 16-resonance spectrum

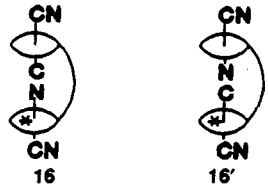

has been established. Two cyanide linkage isomers are formed in the comparable concentrations. (Figure 6, trace d). In the case of mono- and dicyano forms, one of the moieties coordinates cyanide in a preferable manner. The coexisting isomers **13** and **13'** are present at different concentrations (see Figure 6c, Table 2).

The IFe^{III}TTP*o*O(CH$_2$)$_3$O*o*TTPFe^{III}I complex exhibits the similar equilibria and spectral patterns due to cyanide addition as those found for diiron(III) diporphyrin with the shorter link (Table 2). However, form **13** has not been observed. The average shift of the pyrrole resonances of tricyano form **16** has been influenced by the length of a link. The average shifts decreased by 0.5 and 1.9 ppm for the four upfield and four downfield shifted pyrrole resonances, going from the ethylene to the propylene link. The replacement of the counter cation TBA by BPN also produces marked changes of shifts for the tricyano form (Table 2) and is accounted for by interactions in the ionic pair formed. It reflects the structural dissimilarity of cations. The cation related shift differences are more pronounced for one of the diporphyrin subunit, indicating the cation binding preferences.

Temperature Dependencies of Paramagnetic Shifts. The temperature dependencies of the pyrrole chemical shifts for high-spin IFe^{III}TTP*o*O(CH$_2$)$_2$O*o*TTPFe^{III}I and its cyanide adducts are shown in Figure 7. The shifts vary linearly with T^{-1} only for **16** and **17**, but the extrapolated plots do not pass through the position determined for diamagnetic references as found for the tetracyano form **17** (the intercept at 20 ppm) and for one of subunits of tricyano form **16** (the intercept at 15 ppm). The extrapolated positions of four resonances of the second subunit are spread relatively close to the diamagnetic diporphyrin resonance positions (6–9 ppm). The deviation observed for low-spin iron(III) diporphyrins are comparable to those ones for typical monomeric low-spin iron(III) porphyrins.[26]

A Curie plot for the pyrrole resonance of the high-spin complex is consistent with linear behavior in the limited temperature range. The intercept outside the normal diamagnetic position (–20 ppm, Figure 7, trace a) is expected for high-spin iron(III) systems with significant zero-field splitting.[26,31] The dipolar contribution due to the ZFS term is dependent on T^{-2} which usually produces the curvatures of Curie plots.

The set of four pyrrole resonances in the 0 to –5 ppm region, assigned to dicyano species **13** exhibits an anti-Curie behavior (Figure 7, trace b). The respective plots show the decreasing hyperfine shifts with decreasing temperature while all other low-spin species demonstrate the increasing hyperfine shifts with decreasing temperature in accordance with the Curie law.

Cyanide Coordination to Meta- and Para-Linked Diiron(III) Diporphyrins. The ^{1}H NMR spectral changes upon addition of cyanide to IFe^{III}TTP*p*O((CH$_2$)$_3$O*p*TTPFe^{III}I are presented in Figure 8. At low cyanide concentrations two intermediates have been detected as compared to three observed for IFe^{III}TTP*o*O-(CH$_2$)$_2$O*o*TTPFe^{III}I. Trace b of Figure 8 shows the ^{1}H NMR spectrum obtained by addition of 0.6 equiv of cyanide to a solution of a starting high-spin complex. In the downfield region (70 ppm) pyrrole resonances appear resulting from the formation of a monocyano high-spin iron(III) species. The modification of the low-field pyrrole resonance pattern of the substrate upon titration indicates that cyanide addition proceeds in the stepwise manner. The mutual influence of two units of **4** and/or **12** is responsible for the changes in the isotropic shift as related to high-spin halogeno complexes. Further addition of cyanide, up to 1.1:1 cyanide per metal ion, causes the appearance of the resonances in upfield region due to two subunits of tricyano form-(s) with one bridging anion (Figure 8, traces c, d). The resonances are not well-resolved and probably they originate from more than one species. The structures of the bridged complexes result from inter- and intramolecular bridge formation which cannot be distinguished by ^{1}H NMR spectroscopy.

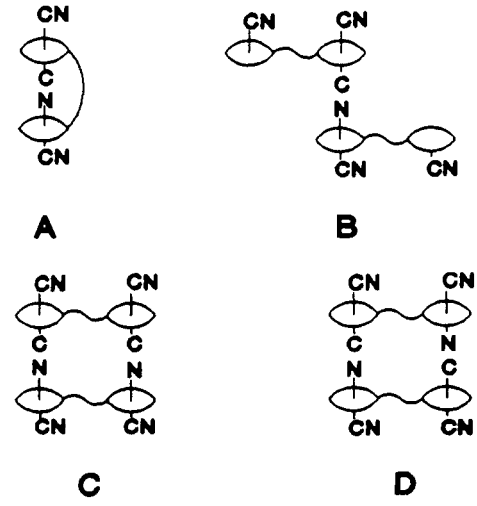

The intramolecular bridged structure A seems to be the most

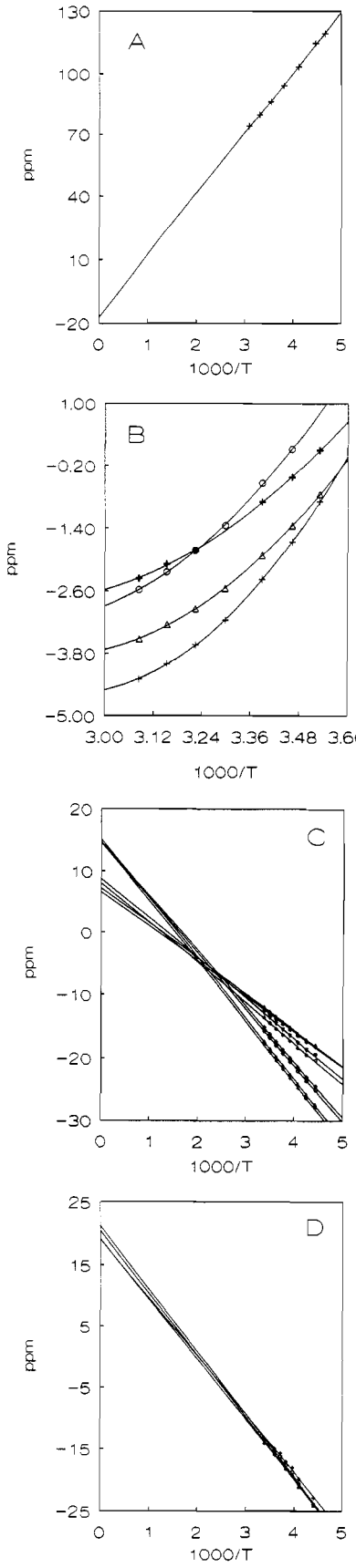

Figure 7. Temperature dependence of pyrrole chemical shifts: (a) high-spin $IFe^{III}TTPoO(CH_2)_2OoTTPFe^{III}I$; (b) $[(CN)Fe^{III}TTPoO(CH_2)_2OoTTPFe^{III}](\mu\text{-CN})$ (**13**); (c) $[(CN)Fe^{III}TTPoO(CH_2)_2OoTTPFe^{III}(CN)](\mu\text{-CN})$ (**16**); (d) $[(CN)_2Fe^{III}TTPoO(CH_2)_2OoTTPFe^{III}(CN)_2](\mu\text{-CN})$ (**17**). Solid lines for a, c, and d show the extrapolation of the experimental data points as expected from the Curie law. The non-Curie temperature dependence is shown for **13**. The solid lines connect the experimental points for trace b only for the sake of presentation.

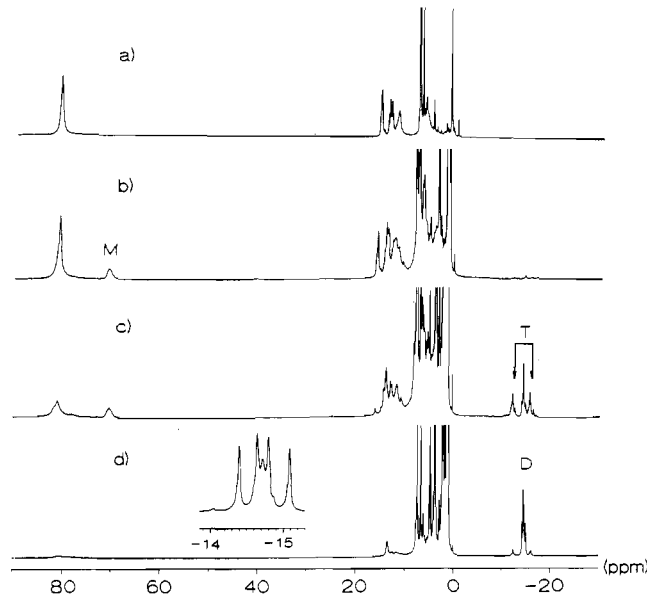

Figure 8. ^1H NMR titration of 4 mM $IFe^{III}TTPpO(CH_2)_2OpTTPFe^{III}I$ with [TBA][CN] (293 K, $CDCl_3$): (a) 0; (b) 0.6; (c) 1.1, and (d) 1.7 equiv of cyanide per metal ion added. Labels of pyrrole resonances: M, monocyanide complex; T, tricyanide, μ-cyanide bridged form(s); D, tetracyanide, dinuclear complex $[(CN)_2Fe^{III}TTPpO(CH_2)_2OpTTPFe^{III}(CN)_2]^{2-}$. The proposed structures of species are discussed in the text.

probable for *ortho* linked diporphyrin complexes, but we discount this structure in the case of *para* linked diporphyrins for steric reasons favoring structure **B**. The hexacyano structures **C** and **D** cannot be ruled out, as well.

Finally, when more than 2 equiv of cyanide per iron(III) are added, the high-field region of the spectrum simplifies and the four pyrrole pattern of **17** prevails (Figure 8, trace d).

Titration of $IFe^{III}TTPmO(CH_2)_3OmTTPFe^{III}I$ produced the similar spectral patterns as those demonstrated for the *para* analog but a larger isotropic shift asymmetry of the diporphyrin subunits was observed.

Cyanide Coordination to (TMP)Fe^{III}I and (TPP)Fe^{III}I. Analysis of diiron(III) diporphyrin complexes in the presence of cyanide allowed us to identify cyanide species not characterized previously for the simple, symmetrical iron(III) tetraphenylporphyrins. We therefore carried out a titration of (TPP)Fe^{III}I and (TMP)Fe^{III}I as the representative examples of monomeric substrates.

The most significant ^1H NMR spectra of undertitrated (TPP)-Fe^{III}I are presented in Figure 9. The formation of $[(CN)Fe^{III}(TPP)]_2(\mu\text{-CN})$ is clearly evidenced by the presence of a pair of pyrrole resonances flanking the peak of $[(TPP)Fe^{III}(CN)_2]$, which remains the only species in solution when the concentration of cyanide reaches twice of that of (TPP)Fe^{III}I (Figure 9). The pyrrole resonance positions of tricyano species correspond to the pyrrole average shifts as determined for two parts of low-spin fragments of $\{[(CN)Fe^{III}TTPoO(CH_2)_2OoTTPFe^{III}(CN)](\mu\text{-CN})\}^-$ (**16**). At the early stage of titration the weak resonance at 70 ppm indicates the formation of (TPP)Fe^{III}(CN). This species exists in a very small concentration. On the other hand, the formation of high-spin (TMP)Fe^{III}(CN) was also observed in early stage of titration, but further addition of cyanide produces only a monomeric low-spin species (TMP)$Fe^{III}(CN)_2$. The steric hindrance of $o\text{-}CH_3$[34] is instrumental in the relative stabilization of the monocyano form and destabilization of the bridged one.

Application of ^1H COSY and ^1H NOESY To Assign Pyrrole Resonances of Low-Spin Forms. Two-dimensional magnitude COSY experiments have been shown to be effective in connecting

(34) Balch, A. L.; Chan, Y.-W.; Cheng, R.-J.; La Mar, G. N.; Latos-Grażyński, L.; Renner, M. W. *J. Am. Chem. Soc.* **1984**, *106*, 7779.

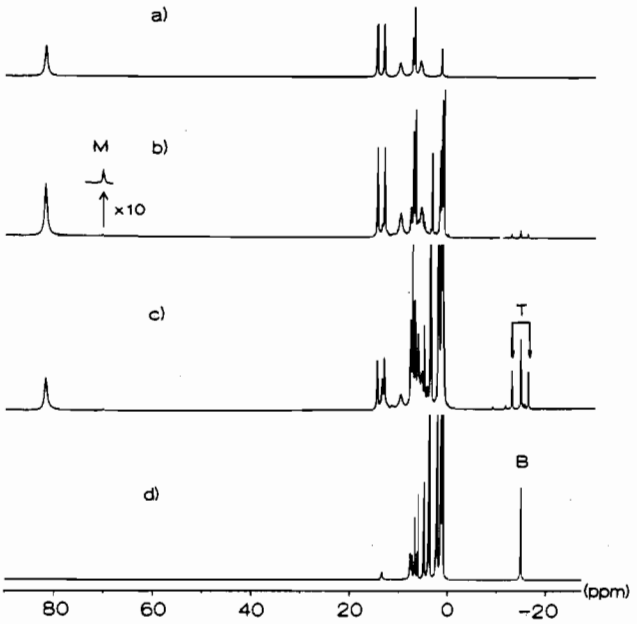

Figure 9. ^{1}H NMR titration of (TPP)Fe^{III}I with [TBA][CN] ($CDCl_3$, 294 K): (a) starting complex; (b) 0.3, (c) 1.1, and ( ) 2.1 equiv of cyanide added per metal ion. Labels of pyrrole resonances: M, monocyanide complex; T, tricyanide, μ-cyanide bridged form; B, $[(TPP)Fe^{III}(CN)_2]^-$. The proposed structures of species are discussed in the text.

within pyrrole couples in low-spin iron(III) complexes of unsymmetrically substituted tetraphenylporphyrins.[35] Within each nonequivalent pyrrole ring of diporphyrins studied in this paper, the pyrrole protons are expected to be coupled with an approximate 5-Hz coupling constant. Figure 10 presents COSY spectra for the selected low-spin cyano iron(III) diporphyrins complexes: $\{[(CN)Fe^{III}TTPoO(CH_2)_2OoTTPFe^{III}(CN)](\mu\text{-}CN)\}^-$; $\{[(CN)Fe^{III}TTPoO(CH_2)_2OoTFTPFe^{III}(CN)](\mu\text{-}CN)\}^-$; $[(CN)_2Fe^{III}TTPoO(CH_2)_2OoTTP^{III}Fe(CN)_2]^{-2}$. Cross-peaks reveal pairwise coupling between two protons located on the same pyrrole ring. The pyrrole spectrum of **16** (eight resonances), obtained during the titration of $IFe^{III}TTPoO(CH_2)_2OoTTPFe^{III}I$ with [TBA][CN], has been tentatively divided into two four-peak sets for which the averaged chemical shifts correspond to positions of two peaks of $[(CN)Fe(TPP)]_2(\mu\text{-}CN)$ (−12.7 and −16.69 ppm vs −13.08 and −16.40 ppm, respectively). Two different coupling patterns have been observed, i.e. 1,3 and 2,4 coupling within the high-field set and 1,2 and 3,4 coupling for the downfield one. (In each set the most high-field pyrrole resonance is labeled 1). The first pattern seems to be typical for iron(III) complexes of unsymmetrically substituted tetraphenylporphyrins;[35] the second pattern is encountered for the first time.

The similar scalar connectivity pattern has been established for unsymmetrical diiron(III) diporphyrin complex (Figure 10, trace b; Table 2). We cannot assign eight-peak sets to particular isomers **16** and **16′** because they exist in similar concentration.

The 1,3 and 2,4 coupling pattern was observed also for all tetracyano species **17** of *ortho*, *meta*, and *para*-linked diporphyrins as presented for the selected *o*-ethylene-bridged complex (Figure 10, trace c). The 1,2 and 3,4 coupling pattern has been found for the *o*-ethylene linked, dicyano complex. This fact might suggests the structure **13** of the complex. Indeed, **13** seems to be precursor of **16**, because only simple addition of cyanide is required for this conversion. From the observed connectivity pattern it is reasonable to propose that 1,3 and 2,4 couplings are

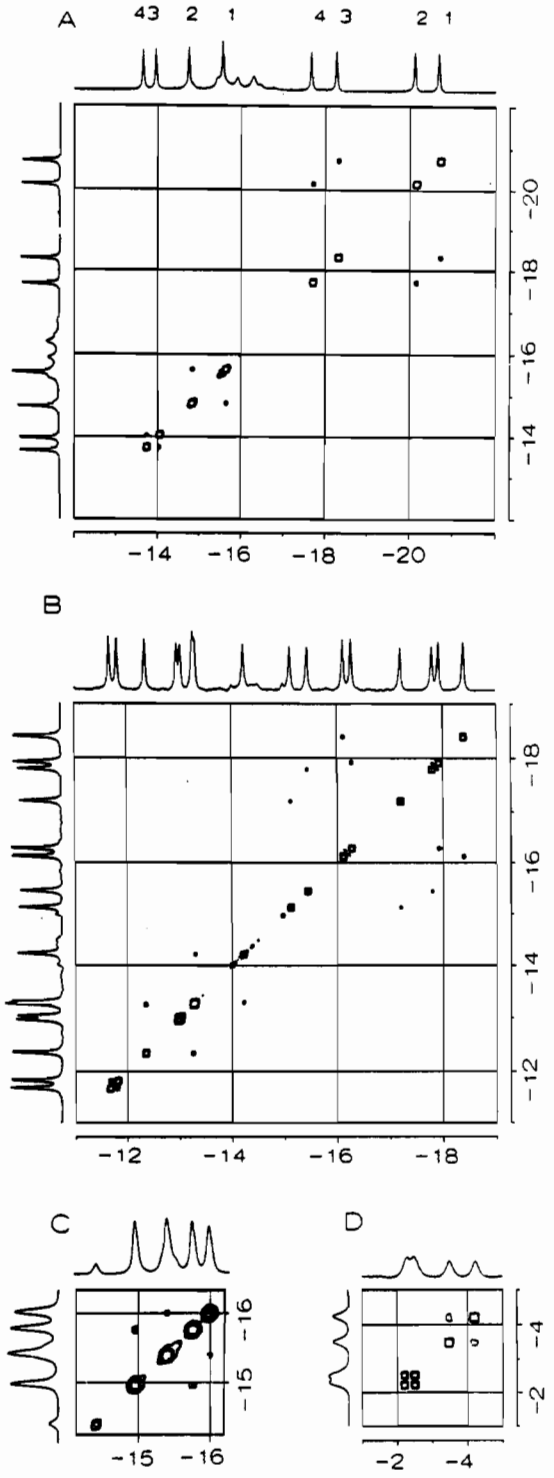

Figure 10. Upfield regions of ^{1}H NMR COSY spectra showing the connectivities within pyrrole resonances of low-spin complexes in chloroform-*d*: (a) $IFe^{III}TTPoO(CH_2)_2OoTTPFe^{III}I$ and [TBA][CN] (1:1 molar ratio, 273.2 K) (**16**); (b) $IFe^{III}TTPoO(CH_2)_2OoTFPFe^{III}I$ and [TBA][CN] (1:1.1 molar ratio, 293 K) (**16** and **16′**); (c) $BrFe^{III}TTPoO(CH_2)_2OoTTPFe^{III}Br$ and (1:2.2 molar ratio, ratio, 278.2 K) (**17**); (d) the same solution as in part a at 323.2 K, (**13**).

characteristic for NC–Fe–CN axial ligation, whereas the 1,2 and 3,4 pattern occurs when CN–Fe–CN axial ligation takes place.

The NOESY experiment has been carried out for the μ-cyanide-bridged species **16**, and the respective maps are presented in Figure 11. In spite of the intrinsic difficulties related to the paramagnetism[35-38] and the relative low concentration of **16** in the equilibrium mixture at 294 K we have observed the following cross-peaks 1,3; 2,4; 1′,2′, and 3′,4′, which are due to NOE cross-

(35) (a) Walker, F. A.; Simonis, U. *J. Am. Chem. Soc.* **1991**, *113*, 8652. (b) Walker, F. A.; Simonis, U. *J. Am. Chem. Soc.* **1992**, *114*, 1929. (c) Lin, Q.; Simonis, U.; Tipton, A. R.; Norvell, C. J.; Walker, F. A. *Inorg. Chem.* **1992**, *31*, 4216. (d) Simonis, U.; Dallas, J.; Walker, F. A. *Inorg. Chem.* **1992**, *31*, 5349.

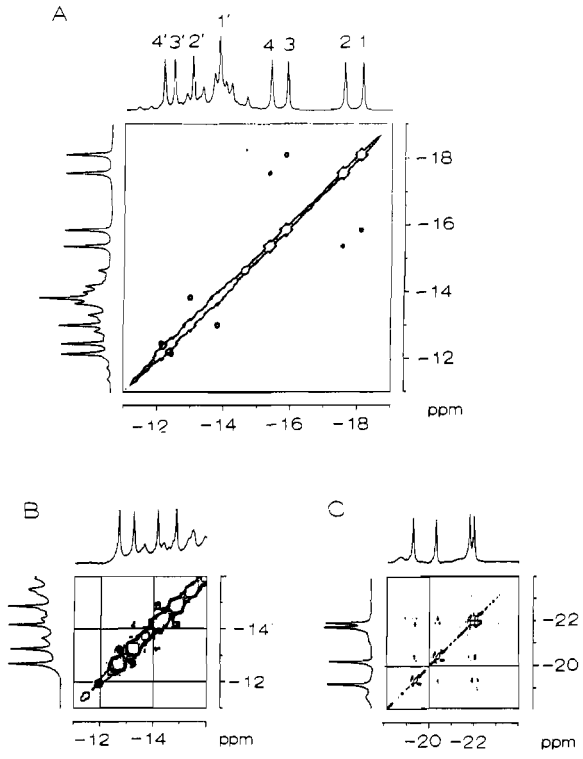

Figure 11. Upfield regions of ^{1}H NMR NOESY spectrum showing the NOE connectivities within pyrrole resonances of the low-spin complex **16** in chloroform-*d* ($IFe^{III}TTPoO(CH_2)_2OoTTPFe^{III}I$ and [TBA][CN], 1:1.3 molar ratio, 294 K, mixing time 30 ms). The inserts B and C present the same region of the NOESY map for the other sample at 257 K, with mixing time 100 ms. Additional cross-peaks between 2′- and 3′-pyrrole protons are observed in the magnitude-processed left part of the 8-peak spectrum (trace B) and between 3- and 4-pyrrole protons in the phase-sensitive processed spectrum (trace C).

relaxation between protons within the same pyrrole ring (Figure 11, trace A). Their scalar connectivities have been determined previously by the COSY experiment. This suggests that protons which gave two additional NOE cross-correlations at 257 K *i.e* 2′,3′ (trace B); and 3,4 (trace C) in the NOESY spectrum are located at two different pyrrole rings, directly flanking the same meso-phenyl ring (see Figure 2).

We have been unable to detect any NOE cross-correlation between protons located on different porphyrins of **16** under the conditions of our experiments.[39] A combination of the 2D NMR experiments allows tentative assignment of the individual pyrrole protons so that 3,4 and 2′,3′ couples correspond to the **b**,**c** and **b**′,**c**′ positions, respectively, as imposed by the complex symmetry. The 2-D coupling pattern, determined for the 1–4 set of pyrrole resonance reflects the spin density distribution expected for the low-spin iron(III) mono-substituted tetraphenylporphyrin in the presence of the one-electron-donating phenyl substituent.[35d,40] In this electronic structure the largest spin densities are expected for **a** and **d** protons and the smallest for the **b** and **c** ones. The assumption has been made that resonance 1 corresponds to the position **a**. This leads to the specific assignment 1 to **a**, 2 to **d**, 3 to **b**, and 4 to **c**.

Analysis of the Electronic Structure of the High-Spin Form. The replacement of the iodide or bromide ligand in high-spin iron(III) porphyrins results in formation of the high-spin monocyano species as concluded based upon the large downfield shift of pyrrole resonances (70 ppm, 293 K). The shift pattern is consistent with the σ-spin density at the pyrrole position. This is reflected by downfield pyrrole shifts and is consistent with the ground electronic state which has an unpaired electron in the σ-symmetry orbital $d_{x^2-y^2}$. The π spin density at meso positions, demonstrated by alternate shifts of phenyl protons implies the delocalization of unpaired spin density from the $d_{xz}d_{yz}$ orbital to the lowest vacant e_g-symmetry orbitals of porphyrin ($4e(\pi^*)$). The paramagnetic shifts of phenyl resonances are in the range reported for high-spin complexes with the smaller contribution of a ZFS mechanism to the dipolar shift.[26,31] The general shift pattern of monocyano species resembles that of high-spin, five-coordinate, σ-bonded (perfluoroaryl)iron(III) porphyrins.[41] Both axial anionic ligands coordinate via carbon atom which seems to be instrumental in decreasing of the equatorial, σ-mechanism contribution, demonstrated by the upfield shift (10 ppm, 293 K) of the pyrrole resonances as compared to the resonances of the halide complexes.

Analysis of the Electronic Structure of Low-Spin Forms. The conversion of high-spin monocyano iron(III) porphyrin to the low-spin state requires an addition of the second axial ligand. The electronic structure of the low-spin complexes $d_{xy}^2(d_{xz}d_{yz})^3$ is reflected in the ^{1}H NMR spectra by the upfield position of the pyrrole resonance(s). The mechanism of the contact shifts involves the porphyrin–iron(III) donation of the electron density to the partially filled set of d_{xz},d_{yz} orbitals. The unpaired electron is delocalized into the $3e(\pi)$ orbitals of porphyrin with the expected maximum spin density at pyrrole positions. The electronic structure of tetracyano forms of diiron(III) diporphyrin fits quite well to the spectral pattern expected for low-spin dicyano complexes of iron(III) porphyrins.[42]

Considering the different electronic structure of the available building blocks the following combinations of the interacting magnetic centers should be considered: (a) high-spin iron(III)–high-spin iron (III); (b) high-spin iron(III)–low-spin iron(III); (c) low-spin iron(III)–low-spin iron(III). Usually the interaction between paramagnetic centers bridged by μ-cyanide is very weak.[43,44] The most effective exchange pathway would result from σ overlap of high-spin iron(III) d_{z^2} orbitals in a tetragonal square-pyramidal ligand field via the σ framework of the cyanide ligand.[45] However, characteristic ^{1}H NMR spectral patterns,

(36) The relaxation times (T_1, T_2) are relatively short in the paramagnetic iron porphyrins which results in the very low intensities of NOE cross peaks, frequently below the practical limit of detection.[35,37,38]

(37) Luchinat, C.; Steurnagel, S.; Turano, P. *Inorg. Chem.* **1990**, *29*, 4351.

(38) (a) Yu, C.; Unger, S. W.; La Mar, G. N. *J. Magn. Reson.* **1986**, *67*, 346. (b) Dugad, L. B.; La Mar, G. N.; Unger, S. W. *J. Am. Chem. Soc.* **1990**, *112*, 1386. (c) Scharberg, M. A.; La Mar, G. N. *J. Am. Chem. Soc.* **1993**, *115*, 6522.

(39) It was found that the intensities of NOESY cross-peaks, determined for low-spin dicyanohemins, increased significantly in the viscous solvents as the ^{1}H–^{1}H cross relaxation increases linearly with viscosity.[38] However, previously explored viscous solvents can be involved in the complex substitution equilibria for the substoichiometric cyanide concentration, required for the formation of **16**. The replacement of chloroform-*d* with a polar solvent would preclude the detection of **16**. Indeed, the tetracyano form **17** was the only species observed for $IFe^{III}TTPo(CH_2)_2OoTTPFe^{III}I$ in the methanol solution.

(40) (a) Walker, F. A.; Benson, M. *J. Phys. Chem.* **1982**, *88*, 3495. (b) Walker, F. A.; Simonis, U.; Zhang, H.; Walker, J. M.; McDonald Ruscitti, T.; Kipp, C.; Ampucht, M. A.; Castillo, B. V., III; Cody, S. H.; Wilson, D. L.; Graul, R. E.; Yong, G. J.; Tobin, K.; West, J. T.; Barichievich, B. A. *New. J. Chem.* **1992**, *16*, 609.

(41) (a) Tabard, A.; Cocolios, P.; Lagrange, G.; Gerardin, R.; Hubsch, J.; Lecomte, C.; Zarembowitch, J.; Guilard, R. *Inorg. Chem.* **1988**, *27*, 110. (b) Kadish, K. M.; Tabard, A.; Lee, W.; Liu, Y. H.; Ratti, C.; Guilard, R. *Inorg. Chem.* **1991**, *30*, 1542.

(42) Małek, A.; Latos-Grażyński, L.; Bartczak, T. J.; Żądło, A. *Inorg. Chem.* **1991**, *30*, 3221 and references cited therein.

(43) (a) Gadet, V.; Bujoli-Doeuf, M.; Force, L.; Verdaguer, M.; El Malkhi, K.; Deroy, A.; Besse, J. P.; Chappert, C.; Veillet, P.; Renard, J.; Beauvillain, P. In *Molecular Magnetic Materials*; Gatteschi, D., Kahn, O., Miller, J. S., Palacio, F., Eds.; NATO ASI Series, Series E; Kluwer: Dordrecht, The Netherlands, 1991; Vol. 1, pp 281–295. (b) Gadet, V.; Mallah, T.; Vedaguer, M.; Veillet, P. *J. Am. Chem. Soc.* **1992**, *114*, 9213.

(44) (a) Gunter, M. J.; Berry, K. J.; Murray, K. S. *J. Am. Chem. Soc.* **1984**, *106*, 4227. (b) Gunter, M. J.; Mander, L. N.; McLaughlin, G. M.; Murray, K. S.; Berry, K. J.; Clark, P. E.; Buckingham, D. A. *J. Am. Chem. Soc.* **1980**, *102*, 1470. (c) Berry, K. J.; Clark, P. E.; Gunter, M. J.; Murray, K. S. *Nouv. J. Chim.* **1980**, *4*, 581.

(45) Ginsber, A. P. *Inorg. Chim. Acta Rev.* **1971**, *5*, 45.

previously shown for antiferromagnetically coupled high-spin iron(III) porphyrins,[26,34,46,47] have not been determined for μ-cyanide-bridged species under investigation. In the case of two low-spin iron(III) centers (c) only the overlap of $d_{xz}d_{yz}$ orbitals can be considered. The π type interaction due to cyanide ligands results in a very small exchange coupling constant J.[43] It may be anticipated that the bridge formation opens a route to weak ferromagnetic/antiferromgnetic interaction(s) between two low-spin iron(III) centers of 16. The temperature dependencies of the isotropic shifts are linear with extrapolation for $T^{-1} \rightarrow 0$ demonstrating only typical deviation from the positions of the diamagnetic standard. The values of intercepts of the low-spin iron(III) porphyrin are mainly due to the dipolar interaction via first- and second-order Zeeman (FOZ, SOZ) mechanisms.[26] Additional contributions to deviations due to the two center interaction are small and can not be deconvoluted from the summaric effect. Structurally analogous μ-alkyl- and μ-aryl-bridged, dinuclear, low-spin iron(III) porphyrin complexes presented also the features characteristic for the negligible, two-center magnetic interactions as determined by ^{1}H NMR spectra.[48]

The pronounced anti-Curie behavior has been observed for four pyrrole resonances of the dicyano form 13 (Figure 7). The second set of resonances is likely located in the rather complex 80 ppm spectral region of high-spin iron(III) porphyrins. The irregular temperature dependence of the isotropic shift can be accounted for by two different mechanisms. The antiferromagnetic coupling between $S = {}^1/_2$ and $S = {}^5/_2$ centers might produce a downfield contribution to the isotropic shift of the low-spin fragment.[49] However, in the extreme case of the strict orthogonality of $d_{xz}d_{yz}$ and d_{z^2} magnetic orbitals the antiferromagnetic interaction should be negligible.[43,44,50] An alternative explanation involves the fast exchange between the bridged and extended dicyano structures.

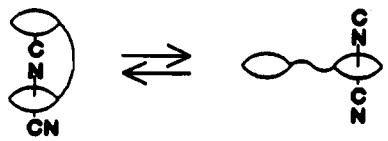

A B

The plot of isotropic shift vs T^{-1} reflects the convolution of two temperature-dependent phenomena i.e. isotropic shift and the fast equilibrium between two isomers.

Conclusion

The observation reported here indicate a consistent pattern of behavior of the diiron(III) diporphyrins upon cyanide ligand addition in chloroform solution. The initial formation of monocyano high-spin complex is found for each iron(III) diporphyrin. The monocyano species can be transformed into the low-spin μ-cyano-bridged diiron(III) complexes of the intra- or intermolecular structure depending on the porphyrin geometry. Addition of excess of cyanide produces complexes with two C-end coordinated cyanide ligands per one iron(III) unit. The characteristic ^{1}H NMR patterns have been assigned to each form in the solution. It is apparent from the ^{1}H NMR investigation that the interactions between paramagnetic centers bridged by μ-cyanide are very weak. The stability of particular forms is readily attributed to steric effects which prohibit the formation of the corresponding μ-cyano-bridged species as in the case of ((TMP)Fe^{III}I or intramolecular for *para*-linked diporphyrins. In the course of our investigation we have established that the similar forms exist for iron(III) porphyrins and iron(III) diporphyrin systems. However, their relative stability is determined by the porphyrin structure. A covalent attachment of two porphyrin increases the local concentration and the likelihood of the internal μ-cyano bridge formation if the porphyrin geometry is appropriate. The apparent stabilization of high-spin monocyano forms (NC)-Fe^{III}TTP*p*O(CH$_2$)$_2$O*p*TTPFe^{III}(CN) as compared to partially low-spin configuration {IFe^{III}TTP*p*O(CH$_2$)$_2$O*p*TTPFe^{III}(CN)$_2$}$^-$ results from entropically favored cyanide distribution.

The structural variability provided by the diporphyrin ligand applied in this work proved to be critical in the directing of the reaction between cyanide and iron(III) porphyrins toward stabilization of the selected cyano species.

Experimental Section

Materials. The porphyrins containing three *p*-methylphenyl and one *o*-, *m*-, or *p*-hydroxyphenyl substituents at meso positions were synthesized according to the method of Little et al.[51]

Pyrrole deuterated 5-(*o*-hydroxyphenyl)-10,15,20-triphenylporphyrin-d_8 was prepared according to a standard procedure.[52]

The hydroxyl substituents were then functionalized by condensation with 1,*n*-dibromoalkanes in dimethylformamide in the presence of potassium carbonate (n = 2 or 3), as previously described.[51,53]

Diporphyrins linked via diether linkage were prepared by reaction of (*o*-, (*m*, or (*p*-(*n*-bromoalkoxy)phenyl)porphyrins obtained in a previous step, with corresponding monohydroxyporphyrins prepared in the first step, in DMF, in the presence of K_2CO_3, in accordance with the published method.[53a] Prolonged reaction time (48 h) and 5–10 molar excess of hydroxyporphyrin were used to drive the reaction toward the formation of diporphyrin. In the case of mixed diporphyrin (H_2TTP*o*O-(CH$_2$)$_2$*o*OTFPH$_2$) the first step of synthesis, i.e. the reaction between 5-(*o*-hydroxyphenyl),10,15,20-tris(*p*-fluorophenyl)porphyrin and excess 1,2-dibromoethane was carried out for 7 days, because of the very low solubility of the porphyrin substrate. The purification procedure was modified for all diporphyrins. The reaction mixture was poured into dichloromethane (1/1 v/v) and DMF was removed from organic phase by a 6-fold extraction with copious amounts of water. Dichloromethane was removed on a rotatory evaporator, and the solid residue was dried overnight. The porphyrins were chromatographed on basic alumina with dichloromethane as eluent. Typically, diporphyrin was eluted as the first band, the excess hydroxyporphyrin substrate was recovered by elution with 4% v/v methanol/dichloromethane. The diporphyrins were characterized by their ^{1}H NMR spectra, which are specified below. The assignments of resonances have been done by 2D COSY experiments (see numbering scheme at Figure 2).

5,10,15-Tri-*p*-tolyl-20-[2-[2-[*o*-(10,15,20-tri-*p*-tolyl-porphinyl)phenoxy]-ethoxy]phenyl]porphyrin [H_2TTP*o*O(CH$_2$)$_2$O*o*TTPH$_2$]. ^{1}H NMR: 8.84 ppm (8H, s, β-pyrrolic); δ_A = 8.73 ppm; δ_B = 8.50 ppm (8H,AB system, J_{AB} = 4.8 Hz, β-pyrrolic); 8.12–8.00 ppm (12H, overlapping three doublets, o_{1-4}); 7.60 ppm (2H, dd, o_5); 7.55–7.45 ppm (12H, overlapping three doublets, m_{1-4}); 6.41 ppm (2H, dd, m_5); 5.87 ppm (2H, d, m_6); 5.80 ppm (2H, ddd, p); 3.33 ppm (4H, s, $CH^{\alpha}_{2(b)}$); 2.70 ppm (6H, s, $CH_{3(1,4)}$); 2.66 ppm (12H, s, $CH_{3(2,3)}$); −2.76 ppm (4H, s, NH).

5,10,15-Tri-*p*-tolyl-20-[2-[3-[*o*-(10,15,20-tri-*p*-tolyl-porphinyl)phenox-y]propoxy]phenyl]porphyrin [H_2TTP*o*O(CH$_2$)$_3$O*o*TTPH$_2$]. ^{1}H NMR: 8.86 ppm (8H, s, β-pyrrolic); δ = 8.74 ppm; δ_B = 8.55 ppm (8H, AB system, J_{AB} = 4.9 Hz, β-pyrrolic); 8.13–8.02 ppm (12H, overlapping three doublets, o_{1-4}); 7.77 ppm (2H, dd, o_5); 7.58–7.50 ppm (12H, overlapping three doublets, m_{1-4}); 6.94 ppm (2H, dd, m_5); 6.59 ppm (2H, ddd, p); 5.82 ppm (2H, d, m_6); 2.77 ppm (4H, t, $CH^{\alpha}_{2(b)}$); 2.70 ppm (12H, s, $CH_{3(2,3)}$); 2.69 ppm (6H, s, $CH_{3(1,4)}$); 0.80 ppm (2H, t, $CH^{\beta}_{2(b)}$); −2.76 ppm (4H, s, NH).

5,10,15-Tri-*p*-tolyl-20-[3-[2-[*m*-(10,15,20-tri-*p*-tolyl-porphinyl)phenoxy]-ethoxy]phenyl]porphyrin [H_2TTP*m*O(CH$_2$)$_3$O*m*TTPH$_2$]. ^{1}H NMR: 8.85

(46) Balch, A. L.; Hart, R. L.; Latos-Grażyński, L. *Inorg. Chem.* **1990**, *29*, 3253.
(47) (a) Phillippi, M. A.; Baenzinger, N.; Goff, H. M. *Inorg. Chem.* **1981**, *20*, 3904. (b) Godziela, G. M.; Ridnour, L. A.; Goff, H. M. *Inorg. Chem.* **1985**, *24*, 1609.
(48) Shin, K.; Yu, B.-S.; Goff, H. M. *Inorg. Chem.* **1990**, *29*, 889.
(49) Banci, L.; Bertini, I.; Luchinat, C. *Struct. Bonding* **1990**, *72*, 113.
(50) Kahn, O. *Struct. Bonding* **1987**, *68*, 89.
(51) Little, R. G.; Anton, J. A.; Loach, P. A.; Ibers, J. A. *J. Heterocycl. Chem.* **1975**, *12*, 343.
(52) Boersma, A. D.; Goff, H. M. *Inorg. Chem.* **1982**, *21*, 581.
(53) (a) Little, R. G. *J. Heterocycl. Chem.* **1978**, *15*, 203. (b) Okamoto, M.; Oishi, N.; Nishida, Y.; Kida, S. *Inorg. Chim. Acta.* **1982**, *64*, L217. (c) D'Souza, F.; Krishnan, V. *Photochem. Photobiol.* **1990**, *51*, 285.

ppm (8H, s, β-pyrrolic); δ = 8.86 ppm; δ_B = 8.82 ppm (8H, AB system, J_{AB} = 4.8 Hz, β-pyrrolic); 8.08 ppm (4H, d, $o_1 + o_4$); 8.02 ppm (8H, d + d, $o_2 + o_3$); 7.79 ppm (2H, dd, o_6); 7.76 ppm (2H, d, o_5); 7.58 ppm (2H, dd, m_5); 7.57 ppm (4H, d, $m_1 + m_4$); 7.48 ppm + 7.42 ppm (4H + 4H, d + d, $m_2 + m_3$); 7.30 ppm (2H, dd, p); 4.40 ppm (4H, t, $CH^{\alpha}_{2(b)}$); 2.72 ppm (6H, s, $CH_{3(1,4)}$); 2.65 ppm (12H, s, $CH_{3(2,3)}$); 2.42 ppm (2H, t, $CH^{\beta}_{2(b)}$); −2.81 ppm (4H, s, NH).

5,10,15-Tri-*p*-tolyl-20-[4-[3-[*p*-(10,15,20-tri-*p*-tolylporphinyl)phenoxy]-propoxy]phenyl]porphyrin [H_2TTP*p*O$(CH_2)_3$O*p*TTPH_2][51a] and 5,10,15-Tri-*p*-tolyl-20-[2-[2-[*o*-(10,15,20-tris(*p*-fluorophenyl)porphinyl)phenoxy]-ethoxy]phenyl]porphyrin [H_2TTP*o*O$(CH_2)_2$O*o*TFPH_2]. ^{1}H NMR: 8.86 ppm (4H, s, β-pyrrolic); 8.81 ppm (4H, s, β-pyrrolic); δ_A = 8.75 ppm; δ_A = 8.64 ppm; δ_B = 8.54 ppm; δ_B = 8.50 ppm (8H, two AB systems, all J_{AB} = 5.0 Hz, β-pyrrolic); 8.20–8.05 ppm (12H, multiplet, o_{1-4}); 7.74–7.39 ppm (14H, multiplet, $o_5 + m_{1-4}$); 6.39 ppm (2H, dd, m_5); 5.89–5.75 ppm (4H, multiplet, m_6 + p); 3.34 ppm (4H, s, $CH_{2(b)}$); 2.72 ppm (3H, s, $CH_{3(1,4)}$); 2.68 ppm (6H, s, $CH_{3(2,3)}$); −2.72 ppm (2H, s, NH); −2.77 ppm (2H, s, NH).

$TMPH_2$. Tetramesitylporphyrin was synthesized by the method of Lindsey and Wagner.[54]

Iron Insertion. The metal ion was inserted to porphyrins by dropwise addition of methanol solution of iron(II) chloride into the refluxing chloroform solution of porphyrin, containing suspended K_2CO_3, under nitrogen atmosphere, in all cases. The reaction mixture was heated about 15 min and exposed to the air, and solvents were removed on a rotatory evaporator. The solid residue was chromatographed on basic alumina with 4% v/v. methanol//dichloromethane mixture. The first eluted band was a μ-oxo dimer(s) of iron(III) porphyrin. The compound was converted into desired halogenate form by 1 h of stirring of the dichloromethane solution of μ-oxo dimer with 0.2 M HCl or 0.4 M HBr (HI) water solution. The methylene dichloride was removed from organic layer on rotary evaporator and the solid residue was dried overnight at 100 °C. No cleavage of diporphyrin was observed in the described synthetic procedure.

Preparation of NMR Samples. The cyanides used throughout these studies were tetrabutylammonium cyanide [TBA][CN] and bis(triphenylphosphine)nitrogen(1+) cyanide [BPN][CN]. The stock solutions of cyanide salts in chloroform-*d* (Glaser AG) were added into an NMR tube containing iron(III) porphyrin complexes via microsyringe. The solvent was purified by passing through basic alumina (activity "0") directly before NMR experiments.

(54) Lindsey, J. S.; Wagner, R. W. *J. Org. Chem.* **1989**, *54*, 828.

Instrumentation. ^{1}H NMR spectra were recorded on a Bruker AMX spectrometer operating at 300 MHz in the quadrature mode.

A typical spectrum was collected over a 45 000 Hz spectral window with 16 K data points, 500–5000 transients for experiment, and a 250-ms prepulse delay. The free induction decay (FID) was apodized using exponential multiplication which induced 5–50-Hz broadening depending on the natural line width.

The residual ^{1}H NMR resonance of the deuterated solvent was used as a secondary reference.

^{2}H NMR spectra were collected using a Bruker AMX instrument operating at 46.1 MHz. A spectral width of 20 kHz was typical using 16 K points. A pulse delay of 50 ms was used. Signal to noise was improved as in ^{1}H NMR spectra. The residual ^{2}H NMR resonance of the solvent was used as a secondary reference.

The COSY spectra were obtained after collecting a standard 1D reference spectrum. The 2D spectra were collected by use of 1024 points in t_2 over desired bandwith (to include all desired peaks) with 258 t_1 blocks and 1024 scans per block. All experiments included four dummy scans prior to the collection of the first block.

Prior to Fourier transformation, the 2D-matrix was multiplied in each dimension with a 30° shifted sine-bell squared window function and zero filled to obtain a 2048 × 2048 word square matrix. NOESY experiments were carried out on a Bruker AMX 300 spectrometer. Both temperature (223–263 K) and mixing time (30–120 ms) were varied to obtain the maximum intensity of cross-peaks. Usually the data were collected over the bandwidth of 15.6 kHz using 1024 complex data points. A total of 512 blocks of 32–256 scans per block were collected depending on the sample concentration. Data were processed with the 30°-phase shifted sine-bell squared window function, zero-filled to 1024 t_1 × 1024 t_2 points prior to Fourier transformation and symmetrization or the magnitude calculation and symmetrization.

Absorption spectra were recorded on a Specord M-42 spectrophotometer.

Infrared spectra were measured with a Bruker IFS113V spectrophotometer in 3-mm path length fluorite cells. The starting porphyrin concentration was 0.015 M.

Acknowledgment. The financial support of the KBN (Grant 2 2651 92 03) is kindly acknowledged.